

**Reaction dynamics of Cl + CH<sub>3</sub>SH : Rotational and vibrational distributions of HCl probed with time-resolved Fourier-transform spectroscopy**

Shin-Shin Cheng, Yu-Jong Wu, and Yuan-Pern Lee

Citation: *The Journal of Chemical Physics* **120**, 1792 (2004); doi: 10.1063/1.1634558

View online: <http://dx.doi.org/10.1063/1.1634558>

View Table of Contents: <http://scitation.aip.org/content/aip/journal/jcp/120/4?ver=pdfcov>

Published by the [AIP Publishing](#)

---

**Articles you may be interested in**

[State-to-state dynamics of the Cl + CH<sub>3</sub>OH HCl + CH<sub>2</sub>OH reaction](#)

*J. Chem. Phys.* **120**, 4231 (2004); 10.1063/1.1644797

[Reaction dynamics of Cl + H<sub>2</sub>S : Rotational and vibrational distribution of HCl probed with time-resolved Fourier-transform spectroscopy](#)

*J. Chem. Phys.* **119**, 4229 (2003); 10.1063/1.1592508

[Ab initio, kinetics, and dynamics study of Cl + CH<sub>4</sub> HCl + CH<sub>3</sub>](#)

*J. Chem. Phys.* **117**, 5730 (2002); 10.1063/1.1497681

[Intramolecular energy flow and nonadiabaticity in vibrationally mediated chemistry: Wave packet studies of Cl + H<sub>2</sub>O](#)

*J. Chem. Phys.* **116**, 1406 (2002); 10.1063/1.1429651

[A four dimensional quantum scattering study of the Cl + CH<sub>4</sub> HCl + CH<sub>3</sub> reaction via spectral transform iteration](#)

*J. Chem. Phys.* **110**, 7233 (1999); 10.1063/1.478627

---



## Re-register for Table of Content Alerts

Create a profile.



Sign up today!



# Reaction dynamics of Cl+CH<sub>3</sub>SH: Rotational and vibrational distributions of HCl probed with time-resolved Fourier-transform spectroscopy

Shin-Shin Cheng and Yu-Jong Wu

*Department of Chemistry, National Tsing Hua University, Hsinchu 30013, Taiwan*

Yuan-Pern Lee<sup>a)</sup>

*Department of Chemistry, National Tsing Hua University, Hsinchu 30013, Taiwan*

*and Institute of Atomic and Molecular Sciences, Academia Sinica, Taipei 106, Taiwan*

(Received 16 September 2003; accepted 27 October 2003)

Rotationally resolved infrared emission spectra of HCl( $v=1-3$ ) in the reaction of Cl+CH<sub>3</sub>SH, initiated with radiation from a laser at 308 nm, are detected with a step-scan Fourier-transform spectrometer. Observed rotational temperature of HCl( $v=1-3$ ) decreases with duration of reaction due to collisional quenching; a short extrapolation to time zero based on data in the range 0.25–4.25  $\mu$ s yields a nascent rotational temperature of  $1150\pm 80$  K. The rotational energy averaged for HCl( $v=1-3$ ) is  $8.2\pm 0.9$  kJ mol<sup>-1</sup>, yielding a fraction of available energy going into rotation of HCl,  $\langle f_r \rangle = 0.10\pm 0.01$ , nearly identical to that of the reaction Cl+H<sub>2</sub>S. Observed temporal profiles of the vibrational population of HCl( $v=1-3$ ) are fitted with a kinetic model of formation and quenching of HCl( $v=1-3$ ) to yield a branching ratio  $(68\pm 5):(25\pm 4):(7\pm 1)$  for formation of HCl( $v=1$ ):( $v=2$ ):( $v=3$ ) from the title reaction and its thermal rate coefficient  $k_{2a} = (2.9\pm 0.7) \times 10^{-10}$  cm<sup>3</sup> molecule<sup>-1</sup> s<sup>-1</sup>. Considering possible estimates of the vibrational population of HCl( $v=0$ ) based on various surprisal analyses, we report an average vibrational energy  $36\pm 6$  kJ mol<sup>-1</sup> for HCl. The fraction of available energy going into vibration of HCl is  $\langle f_v \rangle = 0.45\pm 0.08$ , significantly greater than a value  $\langle f_v \rangle = 0.33\pm 0.06$  determined previously for Cl+H<sub>2</sub>S. Reaction dynamics of Cl+H<sub>2</sub>S and Cl+CH<sub>3</sub>SH are compared; the adduct CH<sub>3</sub>S(Cl)H is likely more transitory than the adduct H<sub>2</sub>SCl. © 2004 American Institute of Physics.  
[DOI: 10.1063/1.1634558]

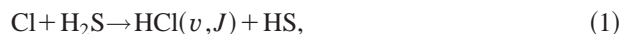
## I. INTRODUCTION

The energy disposal into HX (X=F,Cl,Br) from reactions of halogen atoms with hydrogen-containing species maintains interest because these reactions generate vibrationally excited HX products.<sup>1,2</sup> In these reactions, the newly formed H–X bond carries most of the vibrational excitation, leaving the other product vibrationally cold.

Typical experiments for studying internal energies of HX are performed either with a fast-flow reactor<sup>3</sup> or with a cold-wall flow reactor using the arrested-relaxation technique.<sup>4</sup> A conventional Fourier-transform infrared (FTIR) spectrometer replaces previously employed monochromator or infrared (IR) interference filters to provide improved sensitivity and spectral resolution, but the temporal resolution has been typically in the ms range. In these experiments of bimolecular reactions, rotational quenching is generally non-negligible so that direct detection of products in their nascent rotational distribution is difficult. Observed rotational distributions typically contain substantial low-J components due to quenching; hence the nascent rotational distribution was derived by assuming a Boltzmann distribution and transforming the observed distribution to the high-J envelope to correct for quenching effects.<sup>5</sup> Because of such a limitation,

reported distributions of rotational energies of HX typically have large uncertainties.

In previous work,<sup>6</sup> we employed step-scan time-resolved Fourier-transform spectroscopy (TR-FTS) to investigate the reaction



and derived a nascent rotational distribution of HCl product by a small extrapolation from results determined 0.5–4.0  $\mu$ s after initiation of the reaction with a laser. Our results show a rotational energy of  $8.3\pm 1.5$  kJ mol<sup>-1</sup> HCl, much greater than a value 4.5 kJ mol<sup>-1</sup> reported previously using the arrested relaxation method.<sup>7</sup> The fraction of available energy going into rotation of HCl is  $f_r = 0.12\pm 0.02$ . With added carrier gas to facilitate rotational thermal equilibrium, the temporal evolution of vibrational populations of HCl( $v$ ) recorded with TR-FTS provides information on rates of formation and quenching of HCl( $v$ ), hence the vibrational distribution of the HCl product. A branching ratio of  $0.14\pm 0.01$  for formation of HCl( $v=2$ )/HCl( $v=1$ ) was determined; combining an estimate of the vibrational population of HCl( $v=0$ ) based on a surprisal analysis of previous investigations on the reaction Cl+D<sub>2</sub>S,<sup>8</sup> we reported an average vibrational energy of  $23\pm 4$  kJ mol<sup>-1</sup> for HCl. The fractions of available energy going into vibration of HCl is  $\langle f_v \rangle = 0.33\pm 0.06$ .

<sup>a)</sup> Author to whom correspondence should be addressed. Electronic mail: yplee@mx.nthu.edu.tw; Fax: 886-3-5722892.

According to chemical dynamics of the reaction type X+HY with a heavy–light–heavy mass relationship,<sup>9</sup> the fractions of available energy transforming into vibrational and rotational energies of HX,  $\langle f_v \rangle$  and  $\langle f_r \rangle$ , respectively, should be nearly independent of Y. On the other hand, if available energy were statistically distributed, Y of a more complex structure would compete successfully for energy, leading to HX with less internal energy. In order to understand the effect of the structure of Y on reaction dynamics, we extend investigation of reaction (1) to the reaction



Dill and Heydtmann employed the arrested relaxation method to observe IR chemiluminescence of HCl from reactions (1) and (2a) with a FTIR spectrometer; Cl atoms were produced from microwave-discharged Cl<sub>2</sub>.<sup>7</sup> They observed for reaction (1) emission from only HCl(*v* = 1) with a rotational distribution peaked near *J*' = 4, but for reaction (2a) emission from HCl(*v* = 1 and 2) with rotational distributions peaked at *J*' = 2 and 1, respectively. For reaction (2a), they reported a rotational energy of 5.3 kJ mol<sup>-1</sup> and a ratio of vibrational distributions 0.10:0.90 for HCl(*v* = 2):HCl(*v* = 1), corresponding to an average vibrational energy of 38.3 kJ mol<sup>-1</sup> if the population of HCl(*v* = 0) is assumed to be negligible. The internal energy of the CH<sub>3</sub>S product was uninvestigated.

Nesbitt and Leone<sup>10</sup> detected IR chemiluminescence of HCl to determine the rate coefficient  $k_{2a} = (1.8 \pm 0.4) \times 10^{-10} \text{ cm}^3 \text{ molecule}^{-1} \text{ s}^{-1}$  for reaction (2a); they used S<sub>2</sub>Cl<sub>2</sub> as a source of Cl and initiated the reaction with laser irradiation at 300 nm. More recent measurements on the rate coefficient of reaction (2a) range from  $1.1 \times 10^{-10}$  to  $2.0 \times 10^{-10} \text{ cm}^3 \text{ molecule}^{-1} \text{ s}^{-1}$ .<sup>11,12</sup> Nesbitt and Leone<sup>10</sup> used also Cl<sub>2</sub> as a source of Cl and observed a chain reaction with a length smaller than that expected for reaction (2a), followed by



They also proposed a possible involvement of the reaction



and later determined the rate coefficient to be  $k_{2b} = (4.3 \pm 1.0) \times 10^{-12} \text{ cm}^3 \text{ molecule}^{-1} \text{ s}^{-1}$ .<sup>13</sup> Nicovich *et al.* investigated reaction (2) using Cl<sub>2</sub>CO as a source of Cl; they reported a small negative temperature dependence of *k*<sub>2</sub> and found no kinetic isotope effect when they replaced CH<sub>3</sub>SH with CD<sub>3</sub>SD, indicating that formation of an energized adduct is rate determining.<sup>11</sup> Although both reactions (1) and (2a) have small negative activation energy, only the former shows a substantial kinetic deuterium-isotope effect;<sup>11</sup> hence reaction mechanisms of these two reactions might be different. Comparison of internal state distributions of reaction products from these reactions might provide further information on the details of their reaction mechanism.

Here we report measurements of internal-energy distributions of HCl produced from reaction (2a) by means of TR-FTS in emission mode and compare with those determined for HCl from reaction (1).<sup>6</sup>

## II. EXPERIMENTS

The apparatus employed to obtain time-resolved IR emission spectra has been described previously,<sup>6,14,15</sup> only a brief summary is given here. The photolysis beam from a XeCl laser (308 nm, 41 Hz repetition rate) with a fluence  $\sim 80 \text{ mJ cm}^{-2}$  was employed to photodissociate S<sub>2</sub>Cl<sub>2</sub> to produce Cl atoms to initiate the reaction. Emission of reaction products were collected with a Welsh cell and detected with a step-scan Fourier-transform IR spectrometer equipped with a CaF<sub>2</sub> beamsplitter and an InSb detector. The transient signal of the InSb detector (risetime 0.22 μs) was amplified (bandwidth 1 MHz) before being digitized with either an internal digitizer (16-bit digitizing resolution, 5 μs temporal resolution) or an external data-acquisition board (12-bit digitizing resolution, 25 ns temporal resolution). To decrease the duration of data acquisition, a filter passing 2010–3310 cm<sup>-1</sup> for detection of HCl was used to facilitate undersampling of interferograms. At each scan step data were typically averaged over 60 laser pulses; 6450 scan steps were performed to yield an interferogram resulting in a spectrum of resolution 0.5 cm<sup>-1</sup>.

Typical flow rates and partial pressures are 0.07–0.24 STP cm<sup>3</sup> s<sup>-1</sup> and 0.022–0.075 Torr for CH<sub>3</sub>SH, 0.22–0.45 STP cm<sup>3</sup> s<sup>-1</sup> and 0.070–0.142 Torr for S<sub>2</sub>Cl<sub>2</sub>, and 0.32–4.14 STP cm<sup>3</sup> s<sup>-1</sup> and 0.10–1.30 Torr for Ar; STP implies a standard temperature of 273 K and pressure of 1 atm Ar (Scott Specialty Gases, 99.9995%) and CH<sub>3</sub>SH (AGA Specialty Gases, 99.5%) were used without purification. S<sub>2</sub>Cl<sub>2</sub> (Riedel–de Haën, 99%) was degassed at 180 K before use.

## III. RESULTS AND DISCUSSION

We employed S<sub>2</sub>Cl<sub>2</sub> rather than Cl<sub>2</sub> as a source of Cl atoms because CH<sub>3</sub>S reacts with Cl<sub>2</sub> to propagate chain reactions.<sup>10,16</sup> Photodissociation of S<sub>2</sub>Cl<sub>2</sub> in a molecular beam at 308 nm has been extensively investigated with fragmentation translational spectroscopy.<sup>17</sup> As discussed previously, the average translational energy of Cl atoms immediately after photolysis at 308 nm is 64 kJ mol<sup>-1</sup>, yielding an average collisional energy of 38 kJ mol<sup>-1</sup> between Cl and CH<sub>3</sub>SH.<sup>6</sup> At a pressure of 0.32 Torr, there are more than 12 collisions within 1 μs; hence most Cl atoms are thermalized within 1 μs. At 0 K reactions (2a) and (2b) have enthalpies of reaction  $\Delta H^\circ = -68.2 \text{ kJ mol}^{-1}$  and  $\Delta H^\circ = -42.0 \text{ kJ mol}^{-1}$ , respectively, derived from enthalpies of formation (in kJ mol<sup>-1</sup>) of Cl (119.62),<sup>18</sup> CH<sub>3</sub>SH (-12.12),<sup>19</sup> CH<sub>3</sub>S (131.42),<sup>20</sup> CH<sub>2</sub>SH (157.59),<sup>21</sup> and HCl (-92.13).<sup>18</sup> Hence the available energies for reactions (2a) and (2b) at 298 K are  $\sim 79.4$  and  $53.2 \text{ kJ mol}^{-1}$ , respectively, after taking into account translational and rotational energies of Cl and CH<sub>3</sub>SH; theoretical calculations predict no barrier for reaction (2a).<sup>22</sup> An available energy used for reaction (2a) in previous work was 75 kJ mol<sup>-1</sup>.<sup>7</sup>

Park *et al.* used tunable infrared diode laser to probe the transition Cl(<sup>2</sup>P<sub>1/2</sub>) ← Cl(<sup>2</sup>P<sub>3/2</sub>) and reported that the relative yield of Cl(<sup>2</sup>P<sub>1/2</sub>) is  $0.48 \pm 0.06$  from photolysis of S<sub>2</sub>Cl<sub>2</sub> at 308 nm.<sup>23</sup> The rate coefficient of quenching of Cl(<sup>2</sup>P<sub>1/2</sub>) by Ar is small,<sup>24</sup>  $(3.0 \pm 1.0) \times 10^{-16} \text{ cm}^3 \text{ molecule}^{-1} \text{ s}^{-1}$ , but that by S<sub>2</sub>Cl<sub>2</sub> is much larger. Based on the data of Park

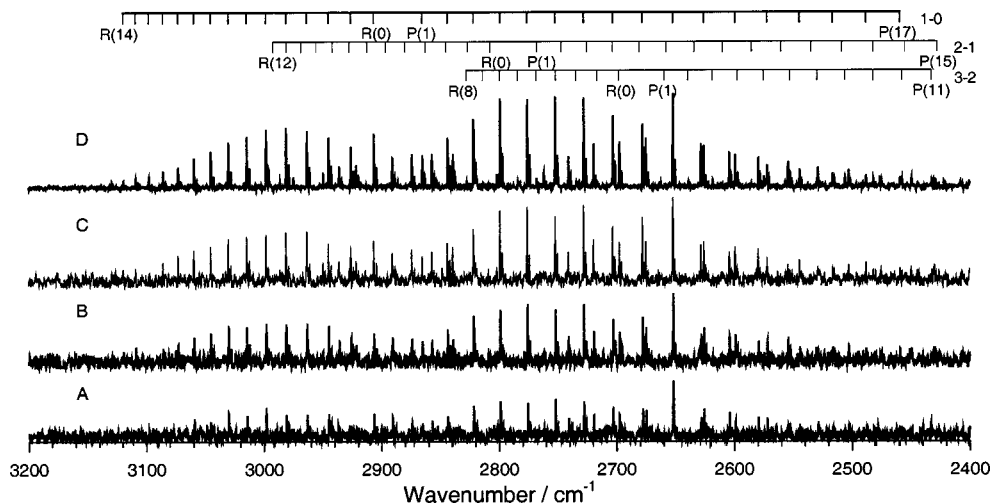


FIG. 1. Infrared emission spectra of HCl in spectral region 2400–3200  $\text{cm}^{-1}$  recorded after irradiation of a flowing mixture of  $\text{S}_2\text{Cl}_2$  (0.142 Torr),  $\text{CH}_3\text{SH}$  (0.075 Torr), and Ar (0.102 Torr) with a XeCl excimer laser at 308 nm. Spectral resolution is  $0.5 \text{ cm}^{-1}$ ; 60 laser pulses were averaged at each scan step. (A) 0.25–0.75  $\mu\text{s}$ ; (B) 0.75–1.25  $\mu\text{s}$ , (C) 1.25–1.75  $\mu\text{s}$ , and (D) 0.25–6.25  $\mu\text{s}$  after laser irradiation. Assignments are shown as stick diagrams;  $J''$  values are listed in parentheses.

*et al.*,<sup>23</sup> with 10 mTorr of  $\text{S}_2\text{Cl}_2$  and 1.99 Torr of Ar in the system, 90% of  $\text{Cl}(^2P_{1/2})$  is quenched within 75  $\mu\text{s}$  after production. In our experiments we employed 142 mTorr of  $\text{S}_2\text{Cl}_2$ ; hence most  $\text{Cl}(^2P_{1/2})$  is expected to be thermalized within 5  $\mu\text{s}$ .

By decreasing the pressure of the reagent as much as possible while maintaining a satisfactory ratio of signal to noise, we recorded emission of HCl with a fast external digitizer at 25-ns resolution, followed by averaging every 20 consecutive time-resolved spectra to yield spectra with temporal resolution of 0.5  $\mu\text{s}$ ; a nascent rotational population of HCl was subsequently derived by short extrapolation to  $t=0$  based on observed population. To determine the vibrational distribution of HCl, we added about 1.3 Torr of Ar to thermalize the rotational distribution and used an internal 16-bit digitizer at 5- $\mu\text{s}$  resolution to obtain temporal profiles of  $\text{HCl}(v)$  up to 500  $\mu\text{s}$  after initiation of reaction. Under experimental conditions ( $t \leq 5 \mu\text{s}$ ) for measurements of rotational distribution of HCl, the presence of excessive  $\text{Cl}(^2P_{1/2})$  might have a small effect on the rotational distribution, whereas for measurements of vibrational distributions ( $t \geq 5 \mu\text{s}$ ),  $\text{Cl}(^2P_{1/2})$  and  $\text{Cl}(^2P_{3/2})$  are thermalized.

#### A. Nascent rotational distribution of $\text{HCl}(v)$

Figure 1 shows emission spectra of HCl recorded 0.25–0.75, 0.75–1.25, 1.25–1.75, and 0.25–6.25  $\mu\text{s}$  after photolysis of a flowing mixture containing  $\text{S}_2\text{Cl}_2$  (0.142 Torr),  $\text{CH}_3\text{SH}$  (0.075 Torr), and Ar (0.102 Torr) at a spectral resolution of  $0.5 \text{ cm}^{-1}$ . Assignments based on spectral parameters reported by Arunan *et al.*<sup>25</sup> and Coxon and Roychowdhury<sup>26</sup> are shown as stick diagrams; notations  $P(J'')$  and  $R(J'')$  are used. Trace C of Fig. 1 shows emission of  $\text{HCl}(v=1)$  with rotational levels  $J'$  up to 16 and weak emission of  $\text{HCl}(v=2$  and 3) with  $J'$  up to 14 and 10, respectively, but at shorter time (such as traces A and B) the poorer signal to noise ratio allows measurements of  $J'$  up to only 15, 12, and 8 for  $\text{HCl}(v=1-3)$ , respectively. A relative population  $P_v(J')$  was derived from intensities of observed

vibration-rotational lines in the  $P$  branch, as described previously.<sup>6</sup> Representative semilogarithmic plots of  $P_v(J')/(2J'+1)$  versus  $J'(J'+1)$  for  $\text{HCl}(v=1)$  are shown in Fig. 2. Data of overlapped lines  $P_v(J')$  for  $v=1$ ,  $J'=3, 4, 6, 10, 11$ , and 13, are not shown. Fitted Boltzmann-type rotational distributions yield rotational temperatures  $1110 \pm 90 \text{ K}$  (0.25–0.75  $\mu\text{s}$ ),  $1100 \pm 70 \text{ K}$  (0.75–1.25  $\mu\text{s}$ ),

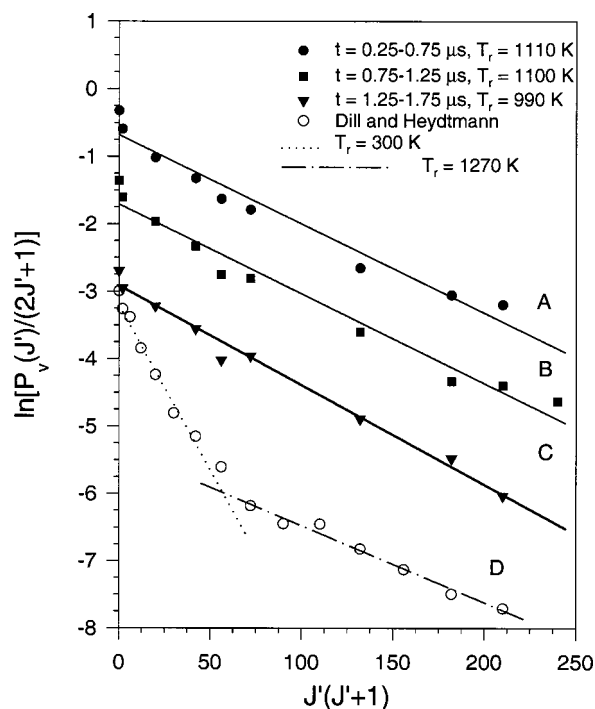


FIG. 2. Semilogarithmic plots of relative rotational populations of  $\text{HCl}(v=1)$  after irradiation of a flowing mixture of  $\text{S}_2\text{Cl}_2$  (0.142 Torr),  $\text{CH}_3\text{SH}$  (0.075 Torr), and Ar (0.102 Torr) with a XeCl excimer laser at 308 nm. (A) 0.25–0.75  $\mu\text{s}$ ; (B) 0.75–1.25  $\mu\text{s}$ , and (C) 1.25–1.75  $\mu\text{s}$  after laser irradiation; data reported by Dill and Heydtman (Ref. 7; symbol  $\circ$ ) are included for comparison. Solid lines represent least-squares fits. For traces (B)–(D) the y-axes are displaced vertically for clarity.

TABLE I. Rotational temperature ( $T_r$ ), rotational energy ( $E_r$ ), and nascent rotational energy ( $E_r^0$ ) of HCl( $v$ ) produced from Cl+CH<sub>3</sub>SH in various reaction periods.

Time/ $\mu$ s	$P=0.32$ Torr				$P=0.81$ Torr			
	$T_r$ /K	$\Sigma_j P_v(J)^a$	$E_r(v)$	$E_r^0(v)^b$	$T_r$ /K	$\Sigma_j P_v(J)^a$	$E_r(v)$	$E_r^0(v)^b$
HCl( $v=1$ )				$E_r^0=8.9\pm 0.4$ kJ mol <sup>-1</sup>				
0.25–0.75	1110 $\pm$ 90	2933	8.1 $\pm$ 0.7	8.4	1070 $\pm$ 60	2792	7.9 $\pm$ 0.5	8.5
0.75–1.25	1100 $\pm$ 70	4691	8.0 $\pm$ 0.6	8.3	1050 $\pm$ 60	4367	7.9 $\pm$ 0.5	8.6
1.25–1.75	990 $\pm$ 70	5942	7.8 $\pm$ 0.6	9.1	920 $\pm$ 90	4907	7.4 $\pm$ 0.8	9.3
1.75–2.25	920 $\pm$ 60	6625	7.4 $\pm$ 0.5	9.3	890 $\pm$ 40	5712	6.9 $\pm$ 0.5	8.9
2.25–2.75	890 $\pm$ 40	7197	7.0 $\pm$ 0.2	8.9	840 $\pm$ 30	6686	6.8 $\pm$ 0.5	9.2
HCl( $v=2$ )				$E_r^0=7.1\pm 0.5$ kJ mol <sup>-1</sup>				
0.25–0.75	1080 $\pm$ 110	1011	6.0 $\pm$ 0.7	6.3	1020 $\pm$ 210	960	6.0 $\pm$ 1.4	6.8
0.75–1.25	1040 $\pm$ 150	1381	5.8 $\pm$ 1.0	6.4	1010 $\pm$ 140	1210	6.1 $\pm$ 1.0	6.9
1.25–1.75	990 $\pm$ 110	1606	5.4 $\pm$ 0.8	6.2	870 $\pm$ 80	1390	5.7 $\pm$ 0.6	7.5
1.75–2.25	850 $\pm$ 80	1815	5.5 $\pm$ 0.6	6.6	850 $\pm$ 110	1765	5.3 $\pm$ 0.8	7.2
2.25–2.75	880 $\pm$ 30	1823	5.8 $\pm$ 0.2	7.5	790 $\pm$ 40	2077	5.4 $\pm$ 0.6	7.7
HCl( $v=3$ )				$E_r^0=4.5\pm 0.4$ kJ mol <sup>-1</sup>				
0.25–0.75	1100 $\pm$ 180	207	3.9 $\pm$ 0.5	4.0	1040 $\pm$ 200	173	3.2 $\pm$ 1.0	3.5
0.75–1.25	1060 $\pm$ 170	232	3.6 $\pm$ 0.5	3.9	970 $\pm$ 150	212	3.7 $\pm$ 0.8	4.3
1.25–1.75	960 $\pm$ 160	272	3.6 $\pm$ 0.6	4.2	900 $\pm$ 140	215	3.4 $\pm$ 0.6	4.3
1.75–2.25	910 $\pm$ 90	294	3.8 $\pm$ 0.3	4.8	850 $\pm$ 100	255	3.7 $\pm$ 0.6	4.9
2.25–2.75	880 $\pm$ 70	308	3.7 $\pm$ 0.3	4.8	790 $\pm$ 80	354	3.6 $\pm$ 0.9	5.2

<sup>a</sup> $P_v(J)$ =(relative integrated emittance)/[(instrumental response factor) (Einstein coefficient)]; arbitrary unit.

<sup>b</sup> $E_r^0=E_r\times(T_r^0/T_r)$ ;  $T_r^0=1150\pm 80$  K.

and  $990\pm 70$  K (1.25–1.75  $\mu$ s) for HCl( $v=1$ ); unless otherwise noted, the uncertainties represent one standard deviation in fitting. Also shown in Fig. 2 is the rotational distribution of HCl( $v=1$ ) reported by Dill and Heydtmann;<sup>7</sup> their results contain two distributions corresponding to temperatures  $\sim 300$  K and  $\sim 1270$  K, with the high- $J$  component having a temperature similar to our measurements. Emission lines associated with HCl( $v=2,3$ ) are treated similarly to derive corresponding rotational temperatures; results are summarized in Table I. Overlapped  $P(J')$  lines are  $J'=4, 5, 6$ , and 11 for  $v=2$ , and  $J'=4, 6$ , and 7 for  $v=3$ .

Rotational distribution of HCl produced via channel (2b) has little effect on our measurements because its rate coefficient is  $<3\%$  of that of reaction (2a). Under our experimental conditions for measurements of rotational distribution of HCl, with a reaction duration of less than 5  $\mu$ s, nearly all HCl is produced from reaction (2a).

Derived rotational temperatures of HCl( $v=1$ ) as a function of reaction periods are shown in Fig. 3 for two total pressures (0.32 and 0.81 Torr). The rotational temperature is smaller at a greater pressure or for a larger reaction period because of quenching. We fitted all data to an exponential decay

$$T_r = 298 + (T_r^0 - 298)\exp(-kt) \quad (4)$$

in which  $T_r^0$  is the nascent rotational temperature and  $k$  is a decay coefficient that varies linearly with pressure. Values  $T_r^0=1180\pm 20$  and  $1150\pm 20$  K were derived for HCl( $v=1$ ) in experiments with pressures of 0.32 and 0.81 Torr, respectively. Similarly, values  $T_r^0=1140\pm 10$  and  $1110\pm 30$  K were derived for HCl( $v=2$ ), and  $T_r^0=1170\pm 20$  and  $1120\pm 10$  K for HCl( $v=3$ ) in experiments at pressures 0.32 and 0.81 Torr, respectively. All rotational temperatures are

similar; an average value  $T_r^0=1145\pm 30$  K is thus obtained. Considering possible errors, we report  $T_r^0=1150\pm 80$  K.

Average rotational energies  $E_r$  for HCl( $v=1-3$ ) are derived on summing a product of level energy and normalized population  $P_v(J)$  for all observed rotational level in each vibrational state; for overlapped lines, the populations are estimated with interpolation based on Boltzmann plots such as the ones in Fig. 2. Nascent average rotational energies  $E_r^0$  are derived on multiplying experimental rotational energies

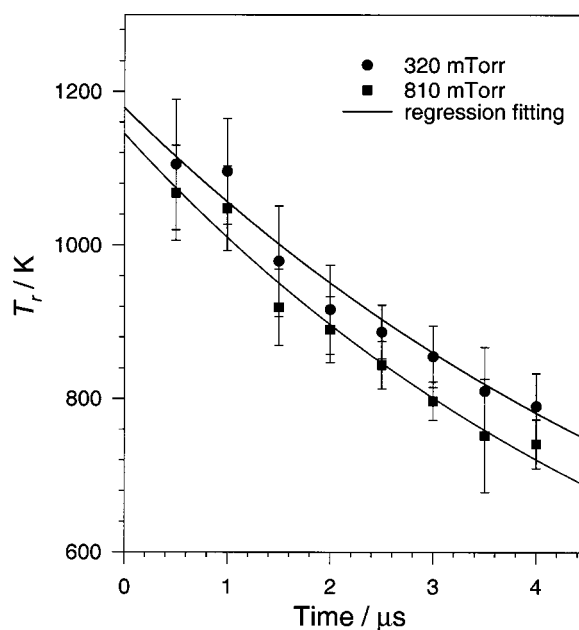


FIG. 3. Variation of rotational temperatures  $T_r$  of HCl( $v=1$ ) as a function of period after irradiation; solid lines represent least-squares fits of Eq. (4); see text.

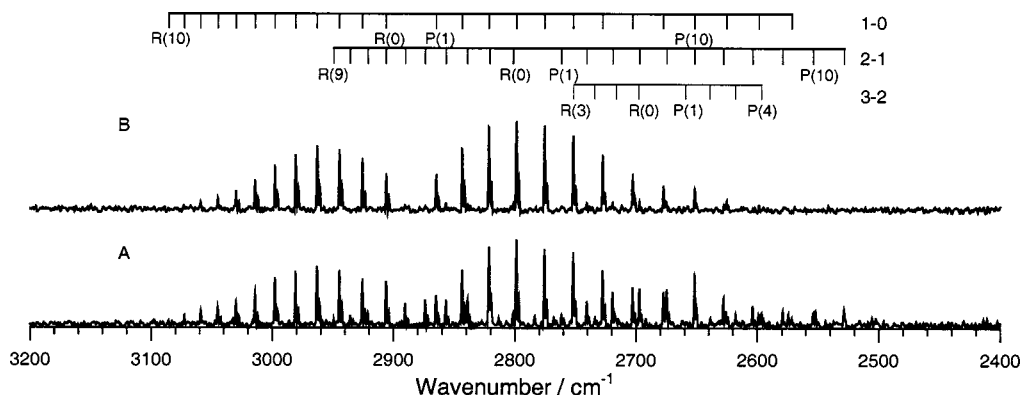


FIG. 4. Infrared emission spectra of HCl in spectral region 2400–3200  $\text{cm}^{-1}$  recorded at 16.9  $\mu\text{s}$  (A) and 201.9  $\mu\text{s}$  (B) after photolysis of a flowing mixture of  $\text{S}_2\text{Cl}_2$  (0.072 Torr),  $\text{CH}_3\text{SH}$  (0.022 Torr), and Ar (1.29 Torr) with a XeCl excimer laser at 308 nm. Spectral resolution is 1.0  $\text{cm}^{-1}$ ; 60 laser pulses were averaged at each scan step. Assignments are shown as stick diagrams.

$E_r$  at each interval by a correction factor  $T_r^0/T_r$ . As Table I shows, this small correction for quenching yields consistent nascent average rotational energies. We average values listed in Table I to obtain  $E_r^0(v) = 8.9 \pm 0.4$ ,  $7.1 \pm 0.5$ , and  $4.5 \pm 0.4$   $\text{kJ mol}^{-1}$  for  $v = 1-3$ , respectively; the decrease in  $E_r^0(v)$  as  $v$  increases is because less rotational levels were observed. An averaged nascent rotational energy  $E_r^0 = 8.2 \pm 0.9$   $\text{kJ mol}^{-1}$  for  $\text{HCl}(v = 1-3)$  was derived on multiplying  $E_r^0(v)$  by its corresponding vibrational population, to be discussed later. The only previous report<sup>7</sup> of  $E_r = 5.3$   $\text{kJ mol}^{-1}$  is about 65% of our value.

The highest rotational level ( $J' = 8$ ) observed for  $\text{HCl}(v = 3)$  lies 9024  $\text{cm}^{-1}$  above the ground state. With the same energy,  $J' = 24$  and 17 of  $\text{HCl}(v = 1)$  and  $\text{HCl}(v = 2)$ , respectively, might be populated. The absence of higher levels in the spectra might reflect limited detectivity. If we assume a Boltzmann distribution and associate extrapolated population with unobserved lines for  $v = 1$  and 2, we derive average rotational energies  $E_r^0(v = 1) = 9.6 \pm 0.3$  and  $E_r^0(v = 2) = 8.7 \pm 0.4$   $\text{kJ mol}^{-1}$ . The average rotational energy of  $\text{HCl}(v = 1-3)$ ,  $E_r^0 = 9.1 \pm 0.9$   $\text{kJ mol}^{-1}$ , should be considered as an upper limit.

## B. Vibrational distribution and rate coefficient

Experiments were carried out with flowing gaseous mixtures containing  $\text{S}_2\text{Cl}_2$  ( $\sim 0.070$  Torr),  $\text{CH}_3\text{SH}$  (0.022–0.042 Torr), and Ar ( $\sim 1.3$  Torr); HCl emission was recorded at 5- $\mu\text{s}$  intervals. Figure 4 shows emission spectra of HCl at a spectral resolution of 1.0  $\text{cm}^{-1}$  recorded at 16.9 and 201.9  $\mu\text{s}$  after photolysis of a flowing mixture containing  $\text{S}_2\text{Cl}_2$  (0.072 Torr),  $\text{CH}_3\text{SH}$  (0.022 Torr), and Ar (1.29 Torr). The signal to noise ratios of these spectra are superior to those recorded for rotational distribution measurements because a 16-bit ADC was used and because more HCl was produced at a later reaction period. We confirmed a nearly thermal ( $\sim 350 \pm 50$  K at 5  $\mu\text{s}$ ) distribution for rotation under these experimental conditions. We averaged results from selective rovibrational  $P(J'')$  lines to yield relative vibrational populations;  $J' = 2, 4-8$  for  $v = 1$ ,  $J' = 2-4, 7, 8$  for  $v = 2$ , and  $J' = 1, 2, 5$  for  $v = 3$  were selected.

Figure 5 shows representative temporal profiles of

$\text{HCl}(v = 1-3)$  obtained upon photolysis of the flowing mixture yielding spectra in Fig. 4. We employed a commercial kinetic modeling program FACSIMILE (Ref. 27) to fit all three temporal profiles collectively according to a model containing the following reactions:

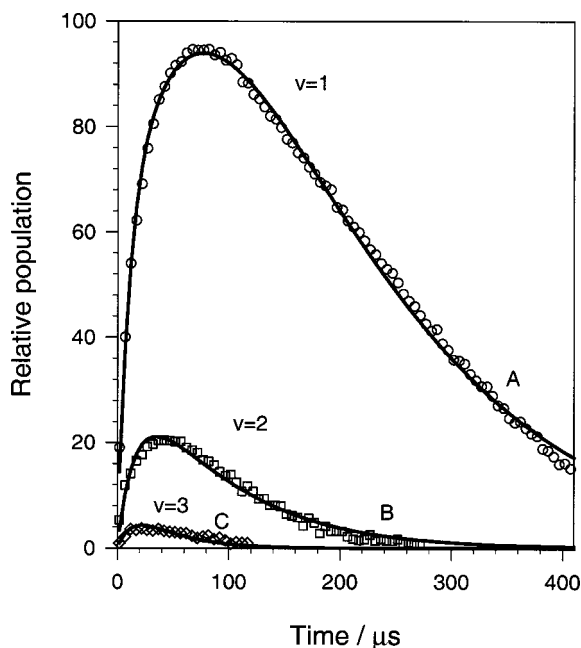
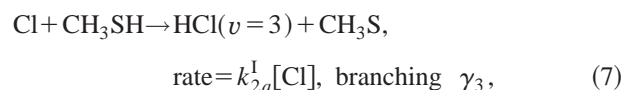
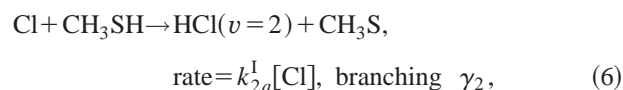
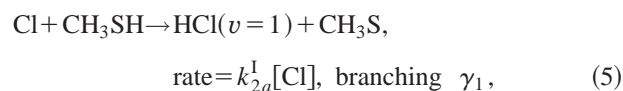
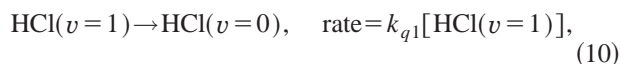
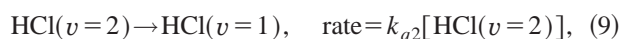
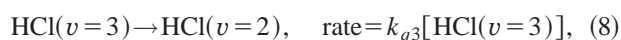
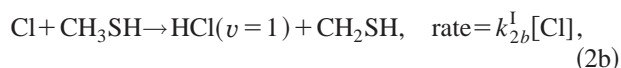


FIG. 5. Temporal profiles of  $\text{HCl}(v)$  recorded after photolysis of a flowing mixture of  $\text{S}_2\text{Cl}_2$  (0.072 Torr),  $\text{CH}_3\text{SH}$  (0.022 Torr), and Ar (1.29 Torr) with a XeCl excimer laser at 308 nm.  $\circ$ ,  $\text{HCl}(v = 1)$ ;  $\square$ ,  $\text{HCl}(v = 2)$ ;  $\diamond$ ,  $\text{HCl}(v = 3)$ .

TABLE II. Experimental conditions and fitted rate coefficients and branching ratios for the reaction Cl+CH<sub>3</sub>SH→HCl(*v*,*J*)+CH<sub>3</sub>S.

Expt. No.	1	2	3	4	5	6
$P_{\text{CH}_3\text{SH}}/\text{mTorr}$	22	25	29	35	39	42
$P_{\text{S}_2\text{Cl}_2}/\text{mTorr}$	72	68	70	69	68	71
$P_{\text{Ar}}/\text{mTorr}$	1290	1320	1300	1280	1320	1310
Laser fluence/ $\text{mJ cm}^{-2}$	77	80	79	78	79	80
% S <sub>2</sub> Cl <sub>2</sub> photolyzed	3.0	3.1	3.1	3.0	3.1	3.1
$k_{q1}/10^4 \text{ s}^{-1}$	0.80±0.02	1.09±0.03	1.31±0.02	1.58±0.07	1.63±0.04	1.59±0.05
$k_{q2}/10^4 \text{ s}^{-1}$	1.29±0.09	1.55±0.10	1.82±0.12	2.22±0.19	2.64±0.10	2.92±0.23
$k_{q3}/10^4 \text{ s}^{-1}$	3.7±0.9	5.2±1.4	7.6±1.3	6.8±2.9	7.7±3.3	8.2±3.4
$k_{2a}^1/10^4 \text{ s}^{-1}$	10.8±0.8	12.6±1.8	25.0±3.2	28.8±3.8	40.0±4.3	40.2±4.1
100 $\gamma_1/(\gamma_1 + \gamma_2 + \gamma_3)$	66±4	66±5	69±9	68±5	70±5	71±6
100 $\gamma_2/(\gamma_1 + \gamma_2 + \gamma_3)$	27±3	26±3	26±3	25±3	23±4	22±3



in which  $k_{2a}^1 = k_{2a} \times [\text{CH}_3\text{SH}]$  and  $k_{2b}^1 = k_{2b} \times [\text{CH}_3\text{SH}]$  are pseudo-first-order rate coefficients, and  $k_{q1} - k_{q3}$  are rate coefficients of vibrational quenching. Reaction (2b) is exothermic to populate only HCl( $v \leq 1$ ). We found that if reaction (2b) were not included in the model, satisfactory fitting for the temporal profile of HCl( $v=1$ ) could not be obtained.

Typically we fit the later portion of temporal profiles with a single exponential decay to derive estimates of  $k_{q1} - k_{q3}$ , followed by fitting all temporal profiles collectively with the above model by keeping  $k_{2b}^1 = 4.3 \times 10^{-12} \text{ cm}^3 \text{ molecule}^{-1} \text{ s}^{-1}$  and estimated  $k_{q1} - k_{q3}$  invariant to derive estimates of  $[\text{Cl}]_0$  (relative value),  $k_{2a}^1$ ,  $\gamma_2/\gamma_1$ , and  $\gamma_3/\gamma_1$ . All parameters except  $k_{2b}^1$  were further optimized to provide the best fit. Values of  $k_{2a}^1$ ,  $\gamma_1/(\gamma_1 + \gamma_2 + \gamma_3)$ ,  $\gamma_2/(\gamma_1 + \gamma_2 + \gamma_3)$ , and  $k_{q1} - k_{q3}$  thus derived under various experimental conditions are listed in Table II; we report an averaged ratio  $\gamma_1:\gamma_2:\gamma_3 = (68 \pm 5):(25 \pm 4):(7 \pm 1)$ , corresponding to the branching  $[\text{HCl}(v=1)]:[\text{HCl}(v=2)]:[\text{HCl}(v=3)]$ . Our observed distribution corresponds to a vibrational temperature greater than that reported by Dill and Heydtmann with  $[\text{HCl}(v=1)]:[\text{HCl}(v=2)] = 9:1$ .<sup>7</sup>

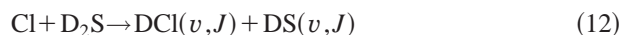
There is no information on the relative population of HCl( $v=0$ ). Dill and Heydtmann<sup>7</sup> assumed that  $[\text{HCl}(v=0)] = 0$  and derived an average vibrational energy of 38 kJ mol<sup>-1</sup>, corresponding to a fraction of available energy (75 kJ mol<sup>-1</sup> used by them) going into the vibration of HCl to be  $\langle f_v \rangle = 0.51$ . If we also assume  $[\text{HCl}(v=0)] = 0$ , we derive an average vibrational energy of 47.4 kJ mol<sup>-1</sup>, about 25% greater than the previous report. However, we think that this assumption likely underestimates the population of HCl( $v=0$ ).

Assuming that available energy does not distribute into vibration of CH<sub>3</sub>S so that the reaction is similar to Cl + H<sub>2</sub>S, and a prior function

$$P^0(f_v) = (1 - f_v)^3 / \Sigma(1 - f_v)^3, \quad (11)$$

in which  $f_v$  is the ratio of the vibrational energy of HCl to the total available energy, we used a surprisal analysis with a model to estimate the vibrational distribution of HCl( $v=0$ ) for reaction (2a) from the observed distribution of HCl( $v=1-3$ ).  $[\text{HCl}(v=0)]/[\text{HCl}(v=1)] \cong 0.22$  is derived to yield a distribution of HCl( $v=0$ ):( $v=1$ ):( $v=2$ ):( $v=3$ ) = (13±2):(59±2):(22±3):(6±1). The distribution yields an average vibrational energy of 41.2±1.0 kJ mol<sup>-1</sup>.

Hossenlopp *et al.*<sup>8</sup> used time-resolved infrared diode laser absorption spectra to probe DCl produced from the reaction



and determined a vibrational distribution of DCl( $v=0$ ):( $v=1$ ):( $v=2$ ) = (33±7):(56±7):(11±3). If we assume that the dynamics of reactions (1), (2a), and (12) are similar and have similar surprisal plots with the cold-DS model (assuming that available energy does not distribute into vibration of DS), we derive a ratio  $[\text{HCl}(v=0)]/[\text{HCl}(v=1)] \cong 0.75$  which yields a vibrational distribution of HCl( $v=0$ ):( $v=1$ ):( $v=2$ ):( $v=3$ ) = (34±2):(45±2):(17±3):(4±1); an average vibrational energy of 31.4±1.0 kJ mol<sup>-1</sup> for HCl is thus derived.

The population of HCl( $v=0$ ) is clearly critical to the determination of average vibrational energy of HCl, but we are unable to obtain this information with the TR-FTS technique. Results from the last two estimates of  $[\text{HCl}(v=0)]$  serve as possible ranges and we take the average of these values, 36±6 kJ mol<sup>-1</sup>, as our estimate, with the error limit covering both values.

### C. Transition state and reaction dynamics of Cl+CH<sub>3</sub>SH and Cl+H<sub>2</sub>S

With the B3LYP/aug-cc-pVTZ density-functional theory<sup>28,29</sup> using the GAUSSIAN 98 program,<sup>30</sup> we performed calculations to locate structures of a transition state (TS1) and an adduct CH<sub>3</sub>S(Cl)H with Cl attaching to the S atom, for the reaction Cl+CH<sub>3</sub>SH. Geometries of the adduct and TS1, and displacement vectors corresponding to imaginary vibrational wave numbers of TS1 predicted with the B3LYP method are shown in Fig. 6. The transition state has a H-Cl bond length of 1.675 Å, smaller than a value of 1.72 Å previously reported by Wilson and Hirst,<sup>22</sup> who employed

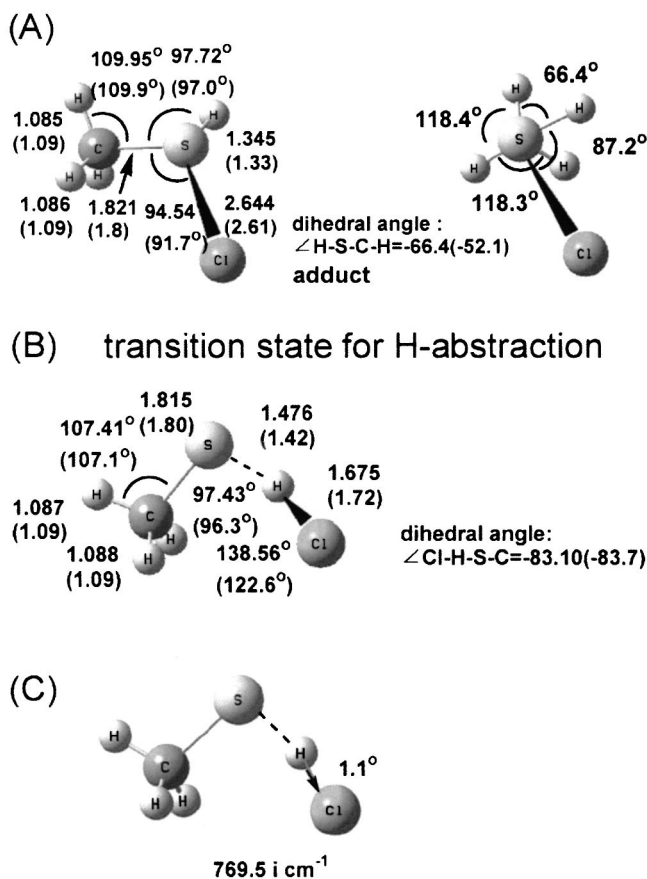


FIG. 6. Geometry of adduct (A) and transition state (B) and its associated vector displacements (C) for the reaction  $\text{Cl} + \text{CH}_3\text{SH}$  predicted with the B3LYP/aug-cc-pVTZ method. Displacement vectors corresponding to imaginary wave numbers are shown with a solid arrow. Bond lengths have unit of Å. Results from Wilson and Hirst (Ref. 22) are listed in parentheses.

the MP2(full)/6-311G\*\* method to predict the transition structure. Their reported molecular parameters are listed parenthetically in Fig. 6 for comparison. The angle of  $\text{Cl-H-S}$ ,  $138.6^\circ$ , predicted in this work is greater than a value  $122.6^\circ$  predicted previously. The displacement vector for motion of the reacting H atom in the reaction coordinate is only  $1.1^\circ$  from the  $\text{H-Cl}$  band. The adduct has an  $\text{S-Cl}$  bond length  $2.644$  Å, slightly greater than a previously reported value of  $2.61$  Å.<sup>22</sup> Predicted vibrational wave numbers are 37.9, 115.1, 223.6, 698.2, 820.3, 933.6, 1035.2, 1323.7, 1346.0, 1459.7, 1463.4, 3051.7, 3132.6, 3147.5, and  $769.5i$   $\text{cm}^{-1}$  for TS1 and 103.3, 139.4, 230.6, 410.0, 692.0, 794.8, 962.9, 1096.8, 1351.5, 1466.0, 1473.2, 2683.2, 3061.6, 3149.4,  $3164.9i$   $\text{cm}^{-1}$  for  $\text{CH}_3\text{S}(\text{Cl})\text{H}$ .

Rate coefficients of both reactions  $\text{Cl} + \text{H}_2\text{S}$  and  $\text{Cl} + \text{CH}_3\text{SH}$  show a small negative temperature dependence,<sup>11</sup> indicating that these reactions proceed via adduct formation. Energies calculated for both reactions with MP4/6-311++G(3df,2p) at geometries optimized with B3LYP/aug-cc-pVTZ are shown in Fig. 7. Calculated exothermicity of  $-61$  and  $-46$   $\text{kJ mol}^{-1}$  for reactions (2a) and (1) at 0 K, respectively, are slightly smaller than experimental values of  $-68$  and  $-58$   $\text{kJ mol}^{-1}$ . At this level of calculation, we could not locate transition states for the direct abstraction path.

We expect that the kinematic effect of the  $\text{Cl-H-S}$  mass

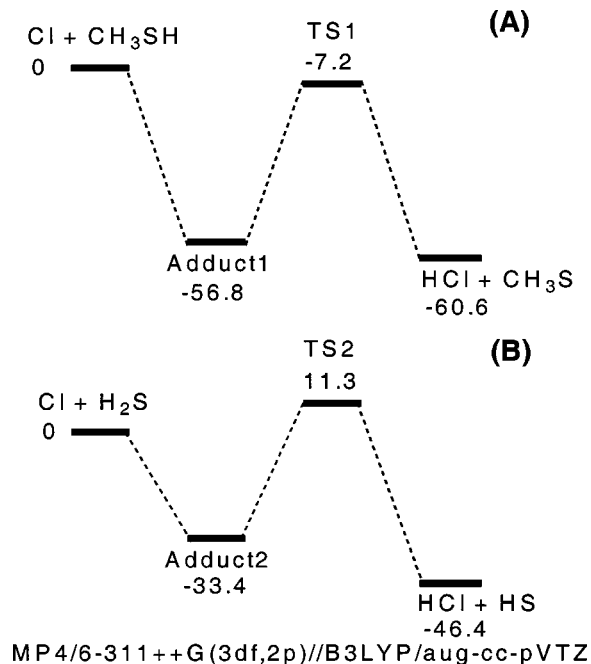


FIG. 7. Potential energies (in  $\text{kJ mol}^{-1}$ ) for reactions  $\text{Cl} + \text{CH}_3\text{SH}$  (A) and  $\text{Cl} + \text{H}_2\text{S}$  (B) calculated with MP4/6-311++G(3df,2p)//B3LYP/aug-cc-pVTZ.

combination is a major factor in determining the internal energies of HCl. The large internal energy of the product HCl is consistent with rapid motion of the reacting H atom, which leaves without interacting with the remainder of the radical fragment  $\text{CH}_3\text{S}$ . Our observation is consistent with such a model. With an available energy of  $79$   $\text{kJ mol}^{-1}$ , the fraction of energy that leads to rotational energy,  $\langle f_r \rangle$ , is  $0.10 \pm 0.02$ . This value is nearly identical to that determined for the reaction between  $\text{Cl} + \text{H}_2\text{S}$ , indicating perhaps a similar kinematic constraint in both reactions.<sup>31</sup> As in the case of  $\text{Cl} + \text{H}_2\text{S}$ , the modified impulse model failed to predict the rotational energy of HCl produced from  $\text{Cl} + \text{CH}_3\text{SH}$ . The small value of  $\alpha = 1.1^\circ$  calculated for the vector of reaction coordinate for TS1 implies little rotational energy for HCl from reaction (2a), in contrast to the experimental observation. The impulse model also fails if we assume that the impulse is exerted along the  $\text{H-S}$  bond of the TS1; according to Eq. (10) in Ref. 6, the torque angle of  $\alpha = 41.4^\circ$  yields a rotational energy  $\sim 33$   $\text{kJ mol}^{-1}$  for HCl.

Kinetic measurements on reaction (2a) showing the absence of a deuterium kinetic isotope effect<sup>11</sup> indicate that the formation of the adduct is rate-determining and the adduct further undergoes rapid reaction to form products. If an adduct  $\text{CH}_3\text{S}(\text{Cl})\text{H}$  is formed initially, rearrangement of the adduct to form  $\text{CH}_3\text{S}$  and HCl is expected to provide greater rotational excitation of HCl than direct abstraction. As a large fraction of available energy is deposited into HCl, we however expect such an adduct to be ephemeral so that substantial redistribution of energy does not occur.

In contrast, even though the rate coefficient of the reaction  $\text{Cl} + \text{H}_2\text{S}$  also has a small negative temperature dependence, it exhibits a substantial kinetic isotope effect with rate coefficient decreasing by a factor of 2 when  $\text{D}_2\text{S}$  replaces

H<sub>2</sub>S.<sup>11</sup> To explain this effect, Nicovich *et al.* suggested that dissociation of the energized adduct back to reactants competes successfully with the H-transfer reaction; when D<sub>2</sub>S replaces H<sub>2</sub>S the rate of the reactive path slows down considerably, whereas the dissociation rate of energized adduct changes little. Our calculations showing TS2~11 kJ mol<sup>-1</sup> above the energy of Cl+H<sub>2</sub>S and TS1~7 kJ mol<sup>-1</sup> below the energy of Cl+CH<sub>3</sub>SH are consistent with this model.

With an available energy of 79 kJ mol<sup>-1</sup>, the fraction of energy that produces vibrational excitation of HCl is  $\langle f_v \rangle = 0.45 \pm 0.08$ , greater than a value of  $\langle f_v \rangle = 0.33 \pm 0.06$  reported for reaction (1);<sup>6</sup> the error limits barely overlap. That reaction of Cl with CH<sub>3</sub>SH produces more vibrational excitation of HCl than that from the reaction of Cl with H<sub>2</sub>S does not conform to a statistical model because CH<sub>3</sub>SH has many more internal degrees of freedom and is hence expected to retain most available energy if the energy were distributed statistically. Our observation of a greater value of  $\langle f_v \rangle$  for reaction (2a) is consistent with the model in which the adduct in reaction (2a) is more transitory than that in reaction (1); energy redistribution is less facile in reaction (2a), hence the other fragment CH<sub>3</sub>S gains little energy. As described in the previous paragraph, our calculations also support that TS1 is more transitory than TS2. Another aspect about the enhanced vibrational excitation of HCl in the reaction Cl + CH<sub>3</sub>SH is that the distance between H and Cl in the transition state, predicted to be 1.675 Å, is greater than the value 1.619 Å predicted for the reaction Cl+H<sub>2</sub>S; the former deviates more from HCl in its equilibrium structure and is expected to be associated with greater vibrational excitation.

To provide more detailed information on this reaction and to compare with experimental results, further theoretical studies on the potential energy surfaces and associated reaction dynamics are needed.

#### D. Rate coefficient of Cl+CH<sub>3</sub>SH→HCl+CH<sub>3</sub>S

Pseudo-first-order rate coefficients  $k_{2a}^I$  derived with model fitting of temporal profiles of vibrational populations of HCl( $v=1-3$ ) are listed in Table II and plotted as a function of [CH<sub>3</sub>SH] in Fig. 8. Although  $k_{2a}^I$  may be derived by fitting the rise of the population of HCl ( $v=3$ ), model fitting with all data provides rate coefficients with less uncertainties. Bimolecular rate coefficients  $k_{2a}$  were derived on fitting an equation

$$k_{2a}^I = k_{2a} \times [\text{CH}_3\text{SH}] + \text{intercept}. \quad (13)$$

A value of  $(2.93 \pm 0.13) \times 10^{-10} \text{ cm}^3 \text{ molecule}^{-1} \text{ s}^{-1}$  is derived. When we fit the data with zero intercept in Eq. (13), we derive  $k_{2a} = (2.99 \pm 0.03) \times 10^{-10} \text{ cm}^3 \text{ molecule}^{-1} \text{ s}^{-1}$ . Considering that errors of  $k_{2a}^I$  in model fitting are ~15% and in measurements of flow rates and pressure are ~3% and 1%, respectively, and that these experiments were not specifically designed for accurate kinetic measurements so that only a small range of [CH<sub>3</sub>SH] was employed, we report a rate coefficient  $k_{2a} = (2.9 \pm 0.7) \times 10^{-10} \text{ cm}^3 \text{ molecule}^{-1} \text{ s}^{-1}$  for reaction (2a), with listed uncertainties representing estimated errors. The value of  $k_{2a}$  derived in this work is slightly

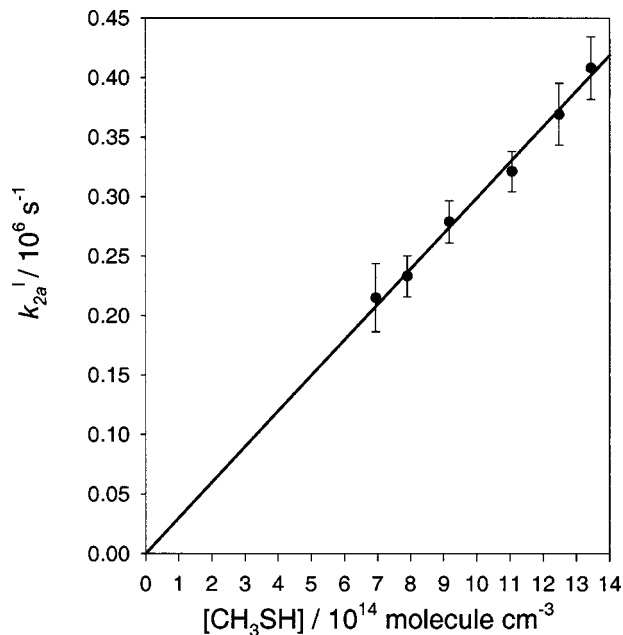


FIG. 8. Plot of pseudo-first-order rate coefficient  $k_{2a}^I$  as a function of [CH<sub>3</sub>SH]; the solid line represents least-squares fitting of data to Eq. (13).

greater than values  $(1.1-2.0) \times 10^{-10} \text{ cm}^3 \text{ molecule}^{-1} \text{ s}^{-1}$  reported previously,<sup>10-12</sup> but with overlapping error limits.

#### IV. CONCLUSION

Rotationally resolved infrared emission of HCl( $v=1-3$ ) is observed with a step-scan Fourier-transform spectrometer in laser-initiated reaction of Cl+CH<sub>3</sub>SH. The average rotational energy and its fraction of partition derived in this work,  $E_r = 8.2 \pm 0.9 \text{ kJ mol}^{-1}$  and  $\langle f_r \rangle = 0.10 \pm 0.01$ , are much greater than in a previous report, but nearly identical to our previous determination for the reaction of Cl+H<sub>2</sub>S. The similarity in rotational energies of HCl product from both reactions indicates that it might be kinematically constrained; the structural complexity of the molecular reactant has little effect on the rotational distribution of HCl produced from its reaction with Cl. The observed vibrational distribution of HCl,  $(v=1):(v=2):(v=3) = (68 \pm 5):(25 \pm 4):(7 \pm 1)$ , and an estimate of  $\langle f_v \rangle = 0.45 \pm 0.08$  indicate more vibrational excitation of HCl than previously reported for this reaction and also for the reaction of Cl+H<sub>2</sub>S. The difference in vibrational excitation is consistent with a difference in predicted H-Cl bond distances in transition structures of these reactions. The pronounced vibrational excitation is also consistent with a more transitory adduct for the reaction Cl + CH<sub>3</sub>SH: kinetic isotope effects observed only for the reaction Cl+H<sub>2</sub>S but not for Cl+CH<sub>3</sub>SH (Ref. 11) are consistent with this picture. Potential energy of the transition state of the reaction Cl+CH<sub>3</sub>SH, but not of Cl+H<sub>2</sub>S, calculated to be smaller than the initial energy of the reactants supports this model. Our time-resolved Fourier-transform spectra have demonstrated improved temporal resolution and detection sensitivity in determining internal-state distributions of

products from bimolecular reactions, especially in measuring nascent rotational distributions that could previously not be determined directly and accurately.

## ACKNOWLEDGMENTS

We thank the National Science Council of Taiwan (Grant No. NSC92-2113-M-007-034) and MOE Program for Promoting Academic Excellence of Universities (Grant No. 89-FA04-AA) for support.

- <sup>1</sup>K. L. Kompa, *Fortschr. Chem. Forsch.* **37**, 1 (1973).
- <sup>2</sup>B. S. Agrawalla and D. W. Setser, *J. Phys. Chem.* **90**, 2450 (1986).
- <sup>3</sup>B. S. Agrawalla and D. W. Setser, in *Gas-Phase Chemiluminescence and Chemi-Ionization*, edited by A. Fontijn (North-Holland, Amsterdam, 1985).
- <sup>4</sup>K. G. Anlauf, P. J. Kuntz, D. H. Maylotte, P. D. Pacey, and J. C. Polanyi, *Discuss. Faraday Soc.* **44**, 183 (1967).
- <sup>5</sup>K. Tamagake, D. W. Setser, and J. P. Sung, *J. Chem. Phys.* **73**, 2203 (1980).
- <sup>6</sup>K.-S. Chen, S.-S. Cheng, and Y.-P. Lee, *J. Chem. Phys.* **119**, 4229 (2003).
- <sup>7</sup>B. Dill and H. Heydtmann, *Chem. Phys.* **35**, 161 (1978).
- <sup>8</sup>J. M. Hossenlopp, J. F. Hershberger, and G. W. Flynn, *J. Phys. Chem.* **94**, 1346 (1990).
- <sup>9</sup>J. C. Polanyi, *Acc. Chem. Res.* **5**, 161 (1972).
- <sup>10</sup>D. J. Nesbitt and S. R. Leone, *J. Chem. Phys.* **72**, 1722 (1980).
- <sup>11</sup>J. M. Nicovich, S. Wang, and P. H. Wine, *Int. J. Chem. Kinet.* **27**, 359 (1995).
- <sup>12</sup>A. Mellouki, J. L. Jourdain, and G. Le Bras, *Chem. Phys. Lett.* **148**, 231 (1988).
- <sup>13</sup>D. J. Nesbitt and S. R. Leone, *J. Chem. Phys.* **75**, 4949 (1981).
- <sup>14</sup>S.-R. Lin and Y.-P. Lee, *J. Chem. Phys.* **111**, 9233 (1999).
- <sup>15</sup>S.-R. Lin, S.-C. Lin, Y.-C. Lee, Y.-C. Chou, I.-C. Chen, and Y.-P. Lee, *J. Chem. Phys.* **114**, 160 (2001).
- <sup>16</sup>M. Braithwaite and S. R. Leone, *J. Chem. Phys.* **69**, 839 (1978).
- <sup>17</sup>Y. R. Lee, C. L. Chiu, and S. M. Lin, *Chem. Phys. Lett.* **216**, 209 (1993).
- <sup>18</sup>M. W. Chase, Jr., *NIST-JANAF Thermochemical Tables*, 4th ed. [J. Phys. Chem. Ref. Data Monogr. **9**, 1 (1998)].
- <sup>19</sup>S. G. Lias, J. E. Bartmess, J. F. Liebman, J. L. Holmes, R. D. Levin, and W. G. Mallrad, *J. Phys. Chem. Ref. Data Suppl.* **17**, 1 (1988).
- <sup>20</sup>J. M. Nicovich, K. D. Kreutter, C. A. van Dijk, and P. H. Wine, *J. Phys. Chem.* **96**, 2518 (1992).
- <sup>21</sup>B. Ruscic and J. Berkowitz, *J. Chem. Phys.* **97**, 1818 (1992).
- <sup>22</sup>C. Wilson and D. M. Hirst, *J. Chem. Soc., Faraday Trans.* **93**, 2831 (1997).
- <sup>23</sup>J. Park, Y. Lee, and G. W. Flynn, *Chem. Phys. Lett.* **186**, 441 (1991).
- <sup>24</sup>G. S. Tyndall, J. J. Orlando, and C. S. Kegley-Owen, *J. Chem. Soc., Faraday Trans.* **91**, 3055 (1995).
- <sup>25</sup>E. Arunan, D. W. Setser, and J. F. Ogilvie, *J. Chem. Phys.* **97**, 1734 (1992).
- <sup>26</sup>J. A. Coxon and U. K. Roychowdhury, *Can. J. Phys.* **63**, 1485 (1985).
- <sup>27</sup>FACSIMILE is a computer software for modeling process and chemical reaction kinetics released by AEA technology, Oxfordshire, United Kingdom.
- <sup>28</sup>A. D. Becke, *J. Chem. Phys.* **98**, 5648 (1993).
- <sup>29</sup>C. Lee, W. Yang, and R. G. Parr, *Phys. Rev. B* **37**, 785 (1988).
- <sup>30</sup>M. J. Frisch, G. W. Trucks, H. B. Schlegel *et al.*, GAUSSIAN 98, Revision A.9, Gaussian Inc., Pittsburgh, Pennsylvania, 1998.
- <sup>31</sup>J. J. Valentini, *J. Phys. Chem.* **106**, 5745 (2002).